Polysiloxane surfactants for the dispersion of carbon nanotubes in non-polar organic solvents

Y. Ji, Y. Y. Huang, A. R. Tajbakhsh, and E. M. Terentjev*

Cavendish Laboratory, University of Cambridge,

J.J. Thomson Avenue, Cambridge CB3 0HE, U.K.

Abstract

We develop two new amphiphilic molecules that are shown to act as efficient surfactants for carbon nanotubes in non-polar organic solvents. The active conjugated groups, which are highly attracted to graphene nanotube surface, are based on pyrene and porphyrin. We show that relatively short (C18) carbon tails are insufficient to provide stabilization. As our ultimate aim is to disperse and stabilize nanotubes in siloxane matrix (polymer and crosslinked elastomer), both surfactant molecules were made with long siloxane tails to facilitate solubility and steric stabilization. We show that pyrene-siloxane surfactant is very effective in dispersing multi-wall nanotubes, while the porphyrin-siloxane is making single-wall nanotubes soluble, both in petroleum ether and in siloxane matrix.

─────────────────
*Electronic address: emt1000@cam.ac.uk

I. INTRODUCTION

With their unique mechanical and electrical properties, and surface chemistry [1, 2], carbon nanotubes (CNTs) have attracted considerable interests in the studies of their fundamental properties as well as the adaption for a wide range of industrial applications. In many situations a homogeneous dispersion of isolated CNTs in solution is required. A bundled CNT system can lead to an uncontrolled alteration in fundamental attributes (e.g. a (n, n) SWNT bundle will display pseudo-semiconducting rather than metallic character [3]), or result in poorer performances (e.g. decrease in the effective stress transfer in composites [4, 5]). Generally, CNTs in big bundles or dense aggregates of other morphology are not very different from ordinary carbon black; for any advanced application one needs them well-separated in a matrix. Unbundling and dispersion of pristine CNTs can be assisted by the use of dispersants or surfactants through non-covalent functionalization. Compared to covalent surface modification of CNTs, non-covalent functionalization has the benefit of preserving the $\pi - \pi$ electronic structures of the outer CNT surfaces. Although a fair amount of research has been conducted on this topic, much of today's surfactants are based on ionic [6, 7, 8] or highly conjugated structures [10, 11, 12], which are mostly suitable for dispersion in aqueous solutions or selected polar solvents (e.g. dimethylformamide, N-methylpyrrolidone, terahydrofluran). The development of a surfactant which can enhance the CNT solubility in generic non-polar organic solvents is of great technical importance especially in the composite fabrication.

An ideal dispersant molecule for CNTs should have an "amphiphilic" structure with an active group attracted towards the graphene wall of a nanotube, and a flexible moiety matching the chemistry of the solubilizing medium and having a carefully chosen size to ensure proportional coverage of the CNT surface. Pyrene and porphyrin are two of the most studied [13, 14, 15, 16] functional groups highly interacting with CNTs. Therefore, the simplest concept to design our ideal dispersant would be to link one of these functional groups to a simple saturated alkyl chain. Such systems based on pyrene/porphyrin derivatives grafted to SWNTs have been studied before [15, 17], however, they did not show remarkable enhancement in CNT solubility in organic solvents. Based on this past experience, we suggest that for stabilizing CNTs in generic solvents, some strict criteria exist for both the CNT-philic and solvent-philic parts of the surfactant.

Although this paper focuses on the CNT dispersion in a generic non-polar solvent, our ultimate aim and interest lie in the nanotube dispersion in silicone matrix. There are many important reasons to produce polymer nanocomposites based on siloxane elastomers, which are highly elastic, chemically stable, insulating materials with a very low glass transition temperature. This explains our use of siloxane moieties in some of our dispersants. However, in order to mix CNTs into siloxane polymers one first needs to assure their miscibility with low-molecular weight solvents, which is what we now proceed to discuss.

We systematically investigated criteria for an effective surfactant to disperse CNTs in non-polar solvents, choosing petroleum ether (PET) as a model. A combination of different active centers (pyrene or porphyrin) and chain attachments (alkyl or siloxane chains) of varying lengths were tested, leading to the successful development of dispersants for SWNTs and MWNTs. Since the nanohybrids formed by integration of pyrene/porhyrin and CNTs have seen promising potential in photovoltaic applications [18], there is an current excitement in these systems; our findings are expected to greatly enhance the processability of these hybrids into useful matrices such as generic silicone elastomers.

II. EXPERIMENTAL

In all cases, the organic synthesis has been an extremely simple one-step process which makes these new materials attractive for practical applications.

A. Pyrene surfactant: mPSi$_{70}$

The core reactants for the synthesis of mono-pyrene siloxane (mPSi$_{70}$) are: polydimethylsiloxane (PDMS) (bis(hydroxyalkyl) terminated, Mn=5600 g/mol, from Aldrich, with an estimated number of siloxane units $n = 70$) and 1-pyrenebutyric acid ($M_w \sim 288$ g/mol, from Aldrich), added in a 1 : 2 ratio. The pyrenebutyic acid powder was first dissolved in dichloromethane (DCM), then mixed with PDMS in the presence of excess N,N-diisopropylcarbondiimide. The reaction mixture was stirred overnight and the solid by-product filtered; the filtrate was then evaporated under reduced pressure to give an oil, which was precipitated from ethanol. The IR spectrum showed a new absorption peak at 1740 cm^{-1} corresponding to the ester group of the butyric acid, thus implying the success-

ful formation of mPSi$_{70}$. The ideal structure of our new surfactant, which we designate as mono-pyrene-siloxane (mPSi$_{70}$), is shown schematically in Table I. The NMR spectrum of the purified product indicated a 9:380 ratio between the protons on the aromatic ring of pyrene ($\sim 7.8 - 8.3$ ppm) and those on the methyl groups of PDMS (~ 0.1 ppm). Each siloxane chain of 70 monomers would have 70*6=420 protons, and there are 9 protons on each pyrene moiety. If we assume the fraction of mono-substituted pyrene-siloxane is x, and thus $(1 - x)$ is the fraction of di-pyrene-siloxane, then the following relation holds: $[9x + 18(1 - x)] : 420 = 9 : 380$. This gives $x = 0.89$, that is, around 10% of the substitution is to form doubly substituted di-pyrene siloxane (dPSi$_{70}$) since we have essentially no un-reacted siloxane. The rest (the majority 90%) is the mono-pyrene siloxane mPSi$_{70}$. The IR and NMR spectra of the mPSi$_7$0 product are available in Supporting information.

Allowing the small proportion of di-pyrene siloxane was intentional (and is the reason for the initial 1:2 ratio of the reactants). First of all, aiming for the strict mono-substitution and have the siloxane/pyrene reacting groups in the 1:1 molar ratio would significantly reduce the reaction yield and make purification more difficult. The excess of un-reacted pyrene is easily washed off by hot ethanol, while the un-reacted PDMS (which would be left if a 1:1 ratio was used) is really hard to separate from pyrene-PDMS. As it was, the reaction yield was above 90% after one day. Secondly, and perhaps more importantly because one might find other ways to improve the yield and purification, we believe that a fraction of di-functional molecules enhance the stability of CNTs at high concentrations by bridging between neighboring tubes. This is no more than an opinion and the reason it is rather subtle: it is based on our earlier experience in rheological studies of dispersed CNTs [19, 20] which indicated that a swollen gel network of effectively crosslinked CNTs has the effect of preventing re-aggregation into compact bundles.

B. Porphyrin surfactant: PhrSi$_{60}$

PDMS (mono(hydroxyalkyl) terminated, Mn=4670 g/mol, from Aldrich, with an estimated number of siloxane units $n =$60) and 5,10,15,20-Tetrakis (4-carboxyphenyl) porphyrin (TPCC, from Aldrich), were added in a 1:16 ratio. The TPCC powder was first dissolved in DCM, then mixed with PDMS in the presence of excess N,N-diisopropylcarbondiimide. The reaction mixture was stirred for two days and the solid by-product filtered; the filtrate was
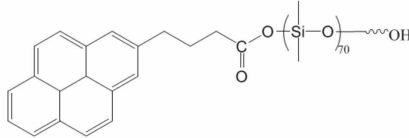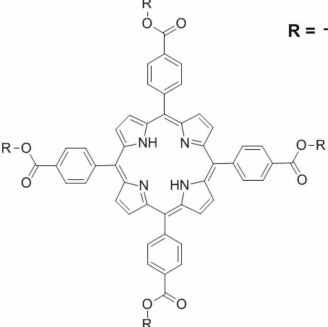
Chemical structure	Symbol	Solubility enhancement for CNTs (in non-polar organic solvent, e.g. PET)
	$mPSi_{70}$	- Effective for MWNTs, but less effective for SWNTs - With mPSi: MWNT (w/w) = 4:1 max. MWNTs solubility in PET > 10mg/ml
R = -(Si-O)$_{60}$	$PhrSi_{60}$	- Effective for SWNTs but not MWNTs - With PhrSi:SWNT (w/w) = 65:1 max. SWNTs solubility in PET > 0.5mg/ml

TABLE I: Summary of the $mPSi_{70}$ and $PhrSi_{60}$ surfactant structures and their effectiveness

then evaporated under reduced pressure to give an oil, which was precipitated in ethanol. The oil was re-dissolved in isopropanol, followed by the addition of appropriate amount of acetone. Subsequently, the mixture was cooled in a freezer, and the dark red layer of the separated product collected. The precipitation procedure described above was repeated several times until there was only one peak remained in gel-permeation chromatography (GPC) analysis. Similar to the mPSi, the IR spectrum (see Supporting Information) showed an absorption peak at 1722 cm^{-1} corresponding to the attachment of ester groups to the porphyrin, implying the successful attachment of siloxane to porphirin. NMR spectrum of the purified product indicated that all of the four carboxyl acid groups of porphyrin have been reacted with PDMS (details in Supporting Information).

- *Short chain porphyrin surfactants: $PhrC_{10}$ and $PhrC_{18}$*

The synthesis process for 5,10,15,20-Tetrakis (n-decoxycarbonyl) porphyrin ($PhrC_{10}$), and 5,10,15,20-Tetrakis (n-octadecoxycarbonyl) porphyrin ($PhrC_{18}$) is similar to that of $PhrSi_{60}$ except that the reactants were different. For $PhrC_{10}$, the reactants were Octadecan-1-ol (1.62 g, 5.99 mmol) and TPCC (0.10 g, 0.12 mmol). For $PhrC_{18}$, the reactants are Decyl alcohol-1-ol (0.95 g, 6 mmol) and TPCC (0.38 g, 0.48 mmol). However, these two surfactants did not give rise to solubility enhancement for either MWNTs and SWNTs in

PET. Therefore, they were not investigated in detail in the present manuscript.

C. Dispersion of carbon nanotubes

Our MWNTs were obtained from Nanostructured & Amorphous Materials, Inc (CVD, purity 95+%, diameter 60-100 nm, as-produced length 5-15 μm), with no functionalization. SWNTs were purchased from Carbon Solutions, Inc., under the P2-SWNT grade (carbonaceous purity of 90%, low functionality and low chemical doping). These SWNTs were grown by electric arc discharge, and consisted of, theoretically, metallic to semiconducting nanotubes in the standard ratio of 1 : 2. The SWNTs were quoted to have bundle length between 500 nm to 1.5 μm, and bundle diameter in the region of 4-5 nm. The Scanning electron micrographs (SEM) of these two two commercial nanotubes sources are shown below in Figs. 3(A) and 4(A). Their purity were further confirmed by thermogravimetric analysis (TGA, results in Supporting Information).

Sonication was employed to assist the dispersion of nanotubes in solution. The effect of sonication on the structural changes of nanomaterials has been recently reviewed in [21], which also includes the analysis of CNT scission induced by ultrasonic energy. Even though in the present study of miscibility we were not particularly concerned about the breakage of nanotubes, due to the excessive power density transmitted into the solution, the sonication conditions were carefully controlled to ensure reproducibility. Ultrasonic Processor (Cole Parmer, 750 W model) with titanium micro-tip was used. The sonication conditions were kept consistent by using standard glass bottles and a fixed cell geometry. The sonication cell has a cooled water bath which kept the ambient temperature of the bottle at 12-16 °C, and also prevented overheating of the solution. The bath water was filled to a constant level throughout the experiments, ensuring that the location of micro-tip emitter and the bottle were both centered within the cylindrically shaped bath. The micro-tip was located at 0.5 cm above the bottom of the bottle and the glass bottle was suspended $\sim$ 4.5 cm above the bath bottom. The following sonication parameter settings were kept the same throughout all experiments: pulsar with 5 s on and 3 s off, probe temperature at 15 °C and vibrational amplitude at 25 %. All sonications were performed with a 1 hr of actual pulsing time. No change in the chemistry of surfactants were found after sonication as determined by absorption spectroscopy (sonochemistry is a known issue in this context [22, 23]). A standard

procedure of dispersion that we followed involved first dissolving the m mass of surfactant into ∼6 ml of PET (petroleum ether, 40-60°C). The solution is then transferred to the holder which contains the n mass of CNTs. The $m : n$ ratios required for different surfactants are shown in Table I. After soaking the CNTs in the surfactant solution overnight, sonication was applied to debundle the nanotubes.

D.   Characterization and data analysis

Thermogravimetric analysis (TGA) of the raw (as-received) CNTs was performed on the TA Instruments Q500 device. Infrared (IR) and Nuclear Magnetic Resonance (NMR) spectroscopy were employed to determine the nature of the reaction products. IR spectra were obtained with Thermo Scientific Nicolet iS10 Spectrometer, and NMR were performed with Bruker Avance 500MHz NMR Spectrometer.

Scanning electron micrographs (SEM) of all CNT samples were obtained on FEI XL30-SFEG high-resolution scanning electron microscope. For the non-surfactant-added reference (see Fig. 3(B)), sonicated MWNTs-PET solution was directly dropped onto mica sheet and the PET was allowed to evaporate in open air. On the other hand, SEM of the sonicated mPSi$_{70}$/MWNT (Fig. 3(C)) required more careful preparation. The sample was prepared by first drop-casting the as-sonicated mPSi$_{70}$/MWNT PET solution onto a mica sheet, after which a few drops of toluene were used to dissolve and wash off the excess mPSi$_{70}$, leaving the residue toluene evaporating in open air.

In order to examine the interaction between the active centers of the surfactants (pyrene or porphyrin) and the nanotube surfaces, absorption spectra of different CNT and surfactant solutions were obtained by CARY 300Bio UV-Vis spectrometer. Absorption peak analysis was performed by OriginPro 8 (V8 SR2, OriginLab) through the "Peak Analyzer" function. Steady-state fluorescence emission measurements were carried out at room temperature using a CARY Eclipse fluorescence spectrophotometer from Varian. For pyrene, the excitation wavelength was 300nm; for porphyrin it was 420nm.

III. RESULTS

Unmodified pyrene, neutral porphyrin, and silicone are all soluble in PET at room temperatures, thus one finds that the synthesized surfactants could all be easily dissolved in PET. However, neither pristine SWNTs or MWNTs demonstrated any solubility in PET. Fast re-aggregation and precipitation of nanotubes was observed immediately after sonication, leaving clear supernatant, e.g. Fig. 1(C).

What happens after adding the surfactants? Following the dispersion procedure described above, we determined the effectiveness of each surfactant by observing the stability of sonicated solutions with different CNT contents and surfactant levels. If no apparent sediment appeared in solution after three days' waiting, the surfactant/CNT combination was considered to be adequate. Table I summarizes the effectiveness of the different surfactants we synthesized.

First of all, no solubility enhancement was found for both SWNTs and MWNTs when $PhrC_{10}$ and $PhrC_{18}$ were used. These two surfactants both result in a pink color when dissolved in PET. Significant decoloration was observed after the surfactant solution was sonicated with SWNTs, but not MWNTs. Since absorption spectroscopy showed no surfactant degradation under our sonication condition, the decoloration phenomenon strongly suggests the adsorption of porphyrin-derived surfactants by SWNTs. By comparing the UV/vis absorption of the sonicated PhrC-PET solution and the sonicated PhrC/SWNTs-PET solution with the same starting PhrC concentration, one finds nearly complete disappearance of the absorption peaks due to PhrC. This further implies the interaction between the porphyrin surfactants and SWNTs, though no solubility enhancement has been observed.

In contrast to the porphyrin with short carbon chain attachments, $mPSi_{70}$ is shown to be a highly effective surfactant for MWNTs, whereas $PhrSi_{60}$ worked well with SWNTs. In the following sections we will bring our focus to these two surfactants, and then discuss the possible reasons for the observed "selective solubilization" effect.

A. $mPSi_{70}$

A remarkable improvement in the solubility of MWNTs in PET was obtained with the addition of $mPSi_{70}$. For SWNTs, however, only a stable suspension of small clusters could

be achieved even when high concentrations of mPSi$_{70}$ were tested. Although these clusters appeared to be stable over a few weeks, mPSi$_{70}$ was not considered to be a good surfactant for SWNTs: our criteria demanded full dispersion. Therefore, we would like to focus our discussion on MWNTs in this section.

Figure 1 compares the results of four samples that underwent different treatments. The MWNTs in sample (A) had been soaked in a few drops of pure mPSi$_{70}$ (which is an oily liquid at room temperature) overnight, after which PET was added to the cluster. By just gentle stirring, some tubes started to diffuse and disperse into PET, resulting in a semi-transparent dark supernatant which remained stable for more than 2 weeks, contrasting in color with the pure surfactant solution shown in sample (B). On the other hand, complete sedimentation was found for MWNTs sonicated in pure PET, illustrated in sample (C). Sample (D) presents a homogeneous mPSi$_{70}$/MWNT solution at a MWNTs concentration of 1 mg/ml, with no visible sedimentation after 2 weeks' standing.

The attachment of mPSi$_{70}$ to MWNTs was strong after sonication treatment, such that the dense sediment obtained after repeated centrifugation (for 40 min at 8000 rpm, which corresponds to acceleration of $\approx 5700\,\mathrm{g}$ in our reactor geometry) and dilution can still be easily re-dispersed. A convenient mPSi$_{70}$:MWNT ratio for the formation of stable solutions was found to be $\sim 4 : 1\,\mathrm{w/w}$ in PET, although a lower ratio of mPSi$_{70}$ to MWNT was also possible. It was found that with the $4 : 1$ mPSi$_{70}$:MWNT standard, over 10 mg/ml (~ 1 wt%) MWNTs in PET could be stabilized, though sediment may appear after three days at very high concentrations. It is expected that this ratio would change depending on the diameter of pristine MWNTs.

The direct interaction between the pyrene group and the CNT was supported by the UV/Vis-absorption spectrum, Fig. 2. It is generally known that MWNTs absorb evenly across UV to near-IR, and the absorbance of pyrene is suppressed when they are anchored to the CNTs [17]. The mPSi$_{70}$ molecule was shown to have similar absorption profile, although slightly red-shifted compared to pure pyrene, with close to zero absorbance in the 370-500 nm region. The complexation between MWNTs and mPSi$_{70}$ (at the standard 4:1 w/w) introduced a steep rise in absorption clearly identifiable in the 370-500 nm region, while the absorption peaks due to free pyrene groups decreased. The anchoring of mPSi$_{70}$ molecules to MWNTs is better demonstrated by comparing the spectra of the standard (4:1) mPSi$_{70}$/MWNTs solution and the similar solution with an excess amount of MWNTs. The

FIG. 1: Bottled samples showing the effect of $mPSi_{70}$: (A) partial solubilization of $mPSi_{70}$ soaked MWNTs in PET without sonication; (B) light-yellow colored $mPSi_{70}$ in PET reference solution; (C) sedimentation of 1 mg/mL MWNTs in PET seen 10 min after sonication; (D) stable 1 mg/mL $mPSi_{70}$/MWNTs in PET solution seen 2 weeks after sonication.

$mPSi_{70}$/MWNTs (excess) solution was prepared at the $mPSi_{70}$:MWNTs ratio of $\sim 3 : 1$, while keeping the overall surfactant concentration in PET constant $[mPSi_{70}] = 5 \times 10^{-5}$ M. By normalizing the absorption of $mPSi_{70}$/MWNTs (excess) at the 370-500 nm region against that of the standard solution, one finds large proportional decrease in the characteristic pyrene absorption bands, Fig. 2(B). This means that the addition of extra nanotubes had caused the $mPSi_{70}$ originally freely dispersed in PET to attach to the additional tube surface. Clearly there exists an equilibrium between the number of anchored $mPSi_{70}$ and the free surfactant molecules in solution. Fluorescence spectroscopy (see Supporting Information) using an excitation wavelength of 300 nm gives further evidence of the interaction between MWNTs and $mPSi_{70}$. The surfactant shows typical fluorescence characteristics of pyrene when dissolved in PET. However, the fluorescence was significantly suppressed in the the presence of MWNTs, which verifies the role of π-stacking due to the direct interaction of pyrene with MWNTs. Since free pyrenes are still present in the solution, the fluorescence is not quenched completely. This effect is different from what was observed for polysoap with pyrene side chains [35], the fluorescence of which could be fully quenched by CNTs. However, the solubility of the CNTs enhanced by $mPSi_{70}$(10 mg/mL) is significantly higher than that achieved by polysoap surfactant (only about 0.075 mg/mL).

To visualize the final state of MWNTs dispersion achieved by the combined effects of sonication and the surfactant, SEM was applied. For the MWNTs reference sample prepared in pure PET, large clusters of MWNTs were observed, Fig. 3(B). In contrast, Fig. 3(C) showing the dispersion assisted by $mPSi_{70}$ indicates that most tubes were isolated and
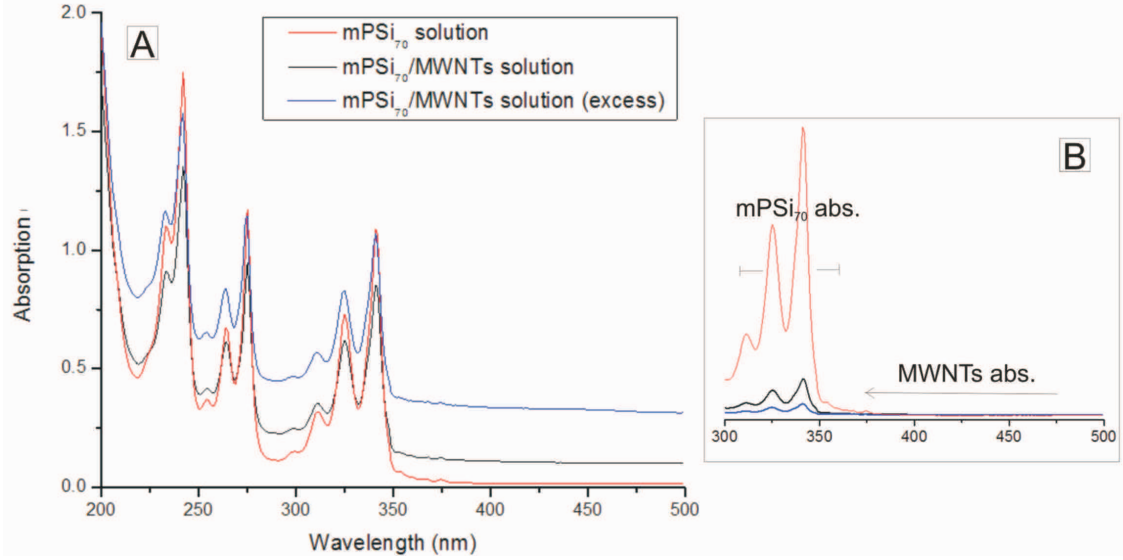
FIG. 2: (A) Absorption spectra of PET solutions of $mPSi_{70}$, the standard 4:1 w/w $mPSi_{70}$/MWNT, and the excess MWNTs/$mPSi_{70}$; (B) the 300-500 nm region selected to emphasize the excess MWNTs absorption curve after normalization against the standard $mPSi_{70}$/MWNT curve. All the absorption spectra were acquired with [$mPSi_{70}$]= 5×10^{-5} M in PET.

well-spaced even after toluene washing away the remaining surfactant. The length of the dispersed tubes has clearly been shortened compared to the quoted 5-15 μm starting values. This is a side effect of sonication which has been quantified in [21]. With 1 hr sonication, most tubes were getting close to the theoretical limiting length L_{lim}; this limiting length was calculated to be $\sim$2-5 μm using the formula $L_{\text{lim}} = \sqrt{d^2\sigma^*/2\eta(\dot{R}_i/R_i)}$ [21], given that the nanotube diameter $d \sim$50-100 nm, the breaking strength $\sigma^* \sim 4$ GPa for CVD MWNTs [24], $\eta \sim 0.01$ Pa.s for typical low-viscosity solvents and $\dot{R}_i/R_i \sim 10^8$ s^{-1} for a cavitation bubble implosion event during sonication (with R_i and $\dot{R}_i$ being the bubble radius and the bubble wall velocity respectively). Well-defined nanotube lengths could only be determined in the surfactant-assisted dispersion in Fig. 3(C), whereas the clustered system of Fig. 3(B) results in spite of shortening of the tubes.

B. PhrSi$_{60}$

The porphyrin-based surfactant PhrSi$_{60}$ was able to effectively solubilize SWNTs but gave only negligible solubility enhancement for MWNTs in PET. The required surfactant to
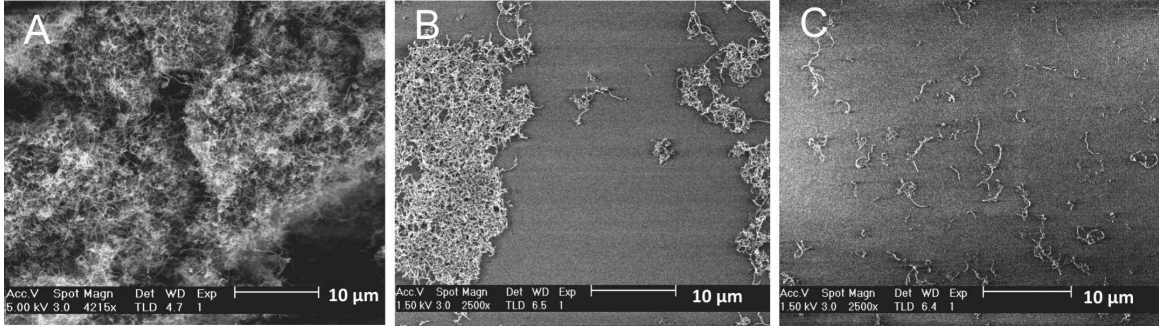
FIG. 3: SEM images showing: (A) as-received MWNTs; (B) clustered MWNTs after sonication in pure PET; (C) well spaced, isolated MWNTs after sonication with mPSi$_{70}$.
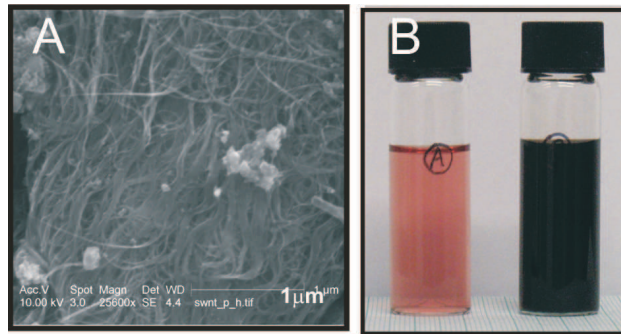

FIG. 4: (A) SEM of as-received SWNTs. (B) Bottled solutions with pure PhrSi$_{60}$-PET on the left hand side, and sonicated 0.15 mg/ml SWNTs-PET solution on the right hand side (PhrSi$_{60}$:SWNTs=65:1 w/w).

CNT ratio was higher for the PhrSi$_{60}$ and SWNT combination; we found that the samples with the ratio $\sim 65 : 1$ performed best. With sonication treatment, a homogeneous solution of up to $\sim$0.5 mg/ml in PET (solubility limit) could be obtained. Figure 4(B) illustrates a pink solution of pure PhrSi$_{60}$ in PET, and a stable 0.15 mg/ml SWNTs solution with PhrSi$_{60}$:SWNT= 65 : 1 (w/w). Compared with the mPSi$_{70}$-MWNT case in the previous section, the stability of SWNTs solution achieved by the use of PhrSi$_{60}$ was not as strong. It was found that the dark supernatant usually remained stable for about two weeks after which precipitation started to appear, while for mPSi$_{70}$/MWNTs, their PET solutions remained fully stable after that time for similar concentration of CNTs.

We again employed absorption spectroscopy to investigate the interaction between the active conjugated group of the surfactant and the CNTs, with results shown in Fig. 5(A). Similar to that of mPSi$_{70}$/MWNTs in PET, one finds an overall increase in baseline absorp-

tion from visible to near-infrared wavelength, indicating the general presence of dark objects (nanotubes in this case) suspended in solution. In addition, the relative decrease in the level of porphyrin absorption is also obvious, for example, in the 1100-1250 and 1300-1500 nm bands. The peak position associated with the Soret transition [25, 26] of $PhrSi_{60}$, i.e. the 416 nm band, remain unchanged. The Q-bands (see insert) at 511 nm, 547 nm seemed to be unaffected by the addition of SWNTs, however, the weaker Q-bands at 593 nm and 649 nm have shifted to 588 nm and 652 nm, respectively. Since some free $PhrSi_{60}$ molecules were still present in solution, the absolute shift in the positions of these minor peaks is expected to be greater after deconvolution. Theoretically, the incorporation of SWNTs should induce additional absorption bands due to the electronic transitions in SWNTs. Although these bands are hard to distinguish in Fig. 5(A), they can be identified in Fig. 5(B), where the difference in absorption between the SWNT and the reference solution is plotted. Since no obvious peaks are identified in the pure $PhrSi_{60}$ and $PhrSi_{60}$/SWNTs solutions in the ~ 850 nm region, the corresponding absorption difference was selected as the reference level. If the level of absorption difference was above this level, it means there is an extra absorption component in addition to the uniform "dark absorption" and the absorption due to $PhrSi_{60}$. Through this data treatment, we identify the unique broad absorption band due to SWNTs at $\sim$950-1110 nm (corresponding to transition centered at ~ 1.2 eV, E_{11}) which is clearly a combination of several absorption peaks. A less obvious band is located in the 700-770 nm region (as determined by Peak Analyzer program, OriginLab) which corresponds to the SWNT E_{22} transition centered at ~ 1.7 eV. The fluorescence of porphyrin was also quenched in the $PhrSi_{60}$-SWNTs complex (data in Supporting Information). Normalized emission spectra of $PhrSi_{60}$-SWNT overlaps with that of the pure $PhrSi_{60}$ in PET. We did not observe shifting of emissions which would occur if the electronic structure of porphyrin were perturbed. Just to note, Casey *et al* [36] also observed similar zero spectrum shift in their porphyrin-SWNT system. Further work is required in order to establish whether electron- or energy transfer could take place between the $PhrSi_{60}$ and SWNTs.

C.   Composite fabrication

The special chemistry of the $mPSi_{70}$ and $PhrSi_{60}$ dangling chains means that they are naturally compatible with PDMS elastomer matrices. Although a growing number of appli-
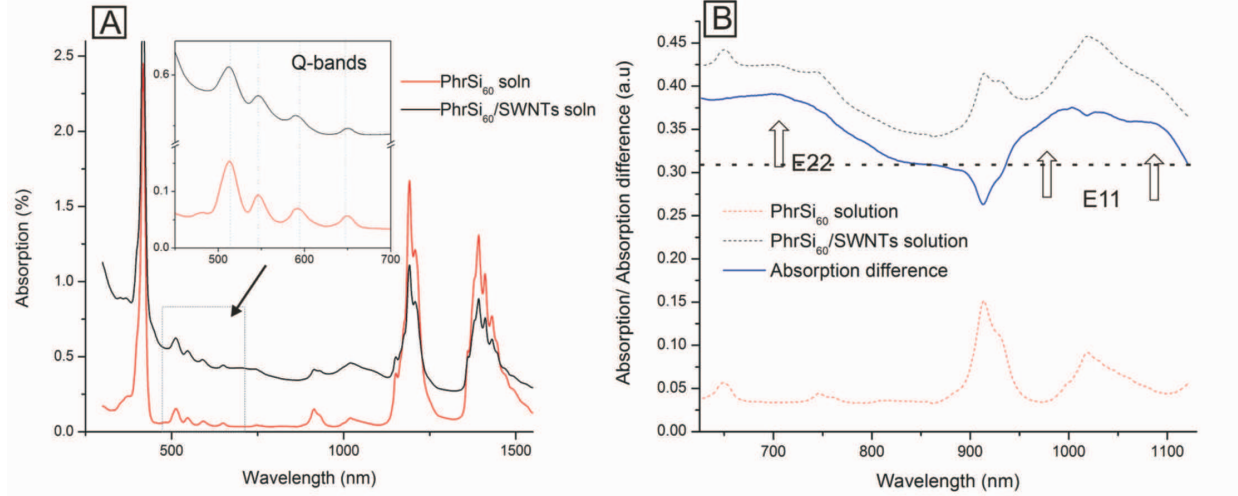
FIG. 5: (A) absorption spectra of PhrSi$_{60}$-PET solution, and that of the sonicated PhrSi$_{60}$/SWNTs solution, with the insert emphasizes the absorption due to Q-band transitions; (B) the difference between pure PhrSi$_{60}$ and PhrSi$_{60}$/SWNT absorption with arrows indicating the regions of absorption bands due to SWNTs.

cations ranging from thermal/fire protections [31] to transparent conductive thin film [33], have been reported for CNT-PDMS composites, the issues associated with CNT dispersion persist. With good stability even at high CNT concentrations, our surfactants (mPSi$_{70}$ for MWNTs, and PhrSi$_{60}$ for SWNTs) can bring two major advantages for the processing of silicone nanocomposites. Firstly, much smaller quantity of solvent is required during solution processing, as opposed to the procedure of Giordani et al[34]. For example, pure PDMS melt (Polydimethylsiloxane, Sylgard 184^{TM} from Dow Corning) could be directly dissolved into the sonicated surfactant/CNT-PET solution at a $\sim 1:4$ PDMS to PET volume ratio to produce a homogeneous composite. The second advantage is that homogeneity in the bulk (3D) structure can be ensured, unlike many cases when only homogeneous 2D film structures produced because of sedimentation. In particular, we were able to shear-align CNTs during casting with associated shear of the top surface, which was then preserved by crosslinking of elastomer matrix. Images of the finished products for higher and lower bounds of concentrations of mPSi$_{70}$/MWNT-PDMS composites are shown as an example in Fig. 6(A). The SEM image in Fig. 6(B) illustrates isolated MWNTs distributed evenly across the fractured surface of a 4 wt% surfactant-stabilized MWNT in PDMS composite. Good interfacial adhesion is found between the nanotube and the matrix. Further study is
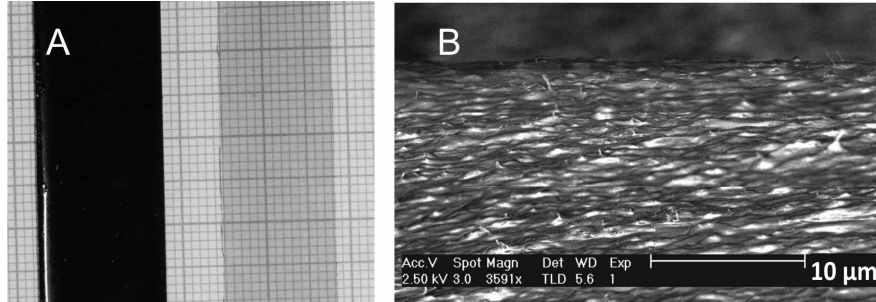
FIG. 6: (A) Examples of 1 mm thick films of mPSi$_{70}$/MWNTs-PDMS composites elastomers on graph paper as background: left-hand-side, 4 wt% MWNT; and right-hand-side 0.06 wt% MWNT. (B) SEM image showing the fractured surface of a 4 wt% mPSi$_{70}$/MWNT-PDMS composite.

focused on testing the electronic and photo-mechanical properties of these composites.

D. Discussion

From the above results it is evident that direct and strong interaction between pyrene or porphyrin moiety and the corresponding CNT surface exists despite one or multiple dangling siloxane chains, each with lengths of n ∼60-70, attached to these active centers. mPSi$_{70}$ and PhrSi$_{60}$ demonstrate interesting selectivity towards the type of nanotubes they can disperse. Interaction between pyrene and CNT surfaces is considered as $\pi - \pi$ stacking in nature [27], thus the local curvature of CNT surface determines the optimum strength of such an interaction because the pyrene group has a rigid planar structure. This gives possible explanation to why the pyrene derived surfactant, mPSi$_{70}$, did not greatly enhance the solubilization of our SWNTs, whose local surface curvature was too high. Although there are reports in the literature [13, 14, 27] claiming unbundling of SWNTs by some pyrene-derived molecules in aqueous solutions, we would like to support the argument that these molecules work better on SWNTs with larger diameters [14]. In future studies, it will be interesting to compare the effectiveness of mPSi$_{70}$ for CNTs of a controlled range of diameters .

However, the above explanation is not applicable to the porphyrin-based surfactant PhrSi$_{60}$. If the entire porphyrin group is seen as the active center, it would exhibit an even wider rigid planar shape than the pyrene moiety. Nevertheless, the resulting PhrSi$_{60}$ surfactant was highly effective for highly curved SWNTs, and ineffective for a much more flat

15

MWNT surface. It has been widely suggested that the donor electrons on the amine group (constituent in porphyrin) could interact favorably with the CNT surface. This is a result of the high curvature of the CNT graphene layers (sp^2 bonds) which renders them electrophilic, and therefore a favorable interaction can take place between electron-accepting CNT surface and a donor molecule via charge transfer/sharing [28, 29]. If these amine groups are the true active sites in the porphyrin moiety, the comparative curvature argument utilized above is no longer relevant. In addition, porphyrin molecules were also found to selectively interact with semi-conducting SWNTs but not the metallic ones [30]. In this sense, one expects that about one-third of the initially dispersed $PhrSi_{60}$/SWNTs were not stable in the solution since the as-received SWNTs should have approximately 1:3 proportion of metallic tubes. This may explain the partial precipitation of SWNTs after two weeks' standing, as well as the ineffectiveness of $PhrSi_{60}$ towards MWNTs (which are all metallic in nature). If confirmed, this effect may offer a new way of separating metallic from semiconducting SWNTs from a bulk sample.

Next we turn our attention to the roles played by the dangling chains of our surfactants. From the above results, it seems that the long siloxane chain is acting much more effectively than the shorter carbon chains. Although molecular-dynamics simulations [31] indicated that siloxane chains can interact favorably with the CNT surfaces through CH-π interaction, we did not find it the case in our experiments. Firstly, our earlier rheological studies [19] revealed that re-aggregation would take place over time even for the initially homogeneous dispersions of CNTs in PDMS. To further prove the "neutrality" between neat siloxane chain and CNTs surface experimentally, pure SWNTs and MWNTs were sonicated in two low-viscosity grade silicone oils (5 cst and 100 cst, Dow Corning 200 Fluid series). The 100 cst silicone oil was suggested to have a molecular weight of $\sim$6000 g/mol [32], similar to that of the siloxane chains attached to pyrene/porphyrin center in our surfactants. Results showed that the sonicated MWNTs exhibited near-complete sedimentation after one day standing in both media. For SWNTs, aggregated clusters of tubes were visible but could remain in suspension for weeks in the more viscous 100 cst silicone oil. A more convincing (and relevant) fact is that we attempted to disperse both kinds of our CNTs in the actual reactant, mono(hydroxyalkyl) terminated PDMS (see the details of $PhrSi_{60}$ synthesis above) and have not detected any solubilization enhancement. We thus conclude that the dangling siloxane chains do not interact favorably with the CNT surfaces. However, as in classical

amphiphilic surfactants, once the active groups are attached to the tubes, the long flexible chains play an important role in "suspending" the tubes in solvent by providing the steric repulsion preventing re-aggregation. Therefore, the length of dangling chains is crucial to dispersion, and we will demonstrate below why a chain length of ∼60-70 was adequate.

If one assumes the siloxane chain grafted to an anchored pyrene/porphyrin group remains in solution taking up an approximate Gaussian coil conformation, the radius of gyration R_g of this dangling part is estimated to be ∼1.3 nm. This is calculated based on $R_g = \sqrt{n}\, a_{\text{SiO}}$ with the number of siloxane units n ∼60-70 and Si-O step length $a_{\text{SiO}} \sim 1.6$ Å. (NB: unlike the "wrapping" mechanism suggested between SWNTs and free PDMS chains in the molecular dynamics simulation of Beigbeder et al[31], we propose that the siloxane part should stay in the surrounding organic solvent for our surfactant molecules with active centers). Firstly, one can notice that the siloxane "coil" provides a barrier just beyond the Van der Waals interaction distance ∼1 nm [9]. Further increase in siloxane chain length may decrease the mobility of the surfactant molecules in solution, reducing the probability of them attaching to the nanotube surface, and also impose lateral packing constraints for the active centers on the surface.

Based on the above considerations we would like to propose that attachment of carbon chains of reasonably long length could also lead to effective solubilization of SWNTs/MWNTs in an organic solvent, to a comparable extent. The main obstacle to test this suggestion lies in the difficulty of synthesizing surfactants with a sufficiently long (n∼70) carbon chains.

IV. CONCLUSIONS

Through separately studying the CNT-affine and solvent-affine parts of a dispersant for non-polar hydrophobic solvents, we conclude that the choice of an active center determines the type of CNT to be dispersed, while the length of the dangling chain determines the final stability of CNT in solution. According to our results, mPSi$_{70}$ was found to effectively disperse MWNTs in PET with solubility over 10 mg/mL, and PhrSi$_{60}$ could enhance the dispersion of SWNTs in PET with a provisional solubility limit of 0.5 mg/ml. Overall, the relatively straightforward process of organic synthesis for all these surfactants make them readily scalable for industrial applications.

Supporting Information Available for this article contains characterization data of thermogravimetric analysis (TGA) of CNTs, NMR and infrared spectra of our surfactants, and the fluorescence spectra of these surfactants on their own and in CNT suspension. This information is available free of charge via the Internet at http://pubs.acs.org/.

---

[1] Dresselhaus, M. S., Dresselhaus, G., and Avouris, P. *Topics in Applied Physics*, **2001**, *80*.

[2] Banerjee, S., Hemraj-Benny, T., and Wong, S. S. *Adv. Mater.*, **2005**, *17*, 17–29.

[3] Delaney, P., Choi, H. J., Ihm, J., Louie, S. G., and Cohen, M. L. *Nature*, **1998**, *391*, 466–468.

[4] Bokobza, L. *Polymer*, **2007**, *48*, 4907–4920.

[5] Shi, D. L., Feng, X. Q., Huang, Y. G. Y., Hwang, K. C, and Gao, H. J. *J. Eng. Mater. Technol.*, **2004**, *126*, 250–257.

[6] Islam, M. F., Rojas, E., Bergey, D. M., Johnson, A. T., and Yodh, A. G. *Nano Lett.*, **2003**, *3*, 269–273.

[7] Zheng, M., Jagota, A., Semke, E. D., Diner, B. A., Mclean, R. S., Lustig, S. R., Richardson, R. E., and Tassi, N. G. *Nature Mater.*, **2003**, *2*, 338–342.

[8] Chen, J., and Collier, C. P. *J. Phys. Chem. B*, **2005**, *109*, 7605–7609.

[9] Shvartzman-Cohen, R., Nativ-Roth, E., Baskaran, E., Levi-Kalisman, Y., Szleifer, I., and Yerushalmi-Rozen, R. *J. Am. Chem. Soc.*, **2004**, *126*, 14850–14857.

[10] Zou, J. H., Liu, L. W., Chen, H., Khondaker, S. I., McCullough, R. D., Huo, Q., and Zhai, L. *Adv. Mater.*, **2008**, *20*, 2055–2060.

[11] Dalton, A. B., Stephan, C., Coleman, J. N., McCarthy, B., Ajayan, P. M., Lefrant, S., Bernier, P., Blau, W. J., and Byrne, H. J. *J. Phys. Chem. B*, **2000**, *104*, 10012–10016.

[12] Cheng, F., Imin, P., Maunders, C., Botton, G., and Adronov, A. *Macromolecules*, **2008**, *41*,

2304–2308.

[13] Chen, R. J., Zhang, Y. G., Wang, D. W., and Dai, H. J. *J. Am. Chem. Soc.*, **2001**, *123*, 3838–3839.

[14] Ehli, C., Rahman, G. M. A., Jux, N., Balbinot, D., Guldi, D. M., Paolucci, F., Marcaccio, M., Paolucci, D., Melle-Franco, M., Zerbetto, F., Campidelli, S., and Prato, M. *J. Am. Chem. Soc.*, **2006**, *128*, 11222–11231.

[15] Satake, A., Miyajima, Y., and Kobuke, Y. *Chem. Mater.*, **2005**, *17*, 716–724.

[16] Li, H., Zhou, B., Gu, L., Wang, W., Shiral Fernando, K. A., Kumer, S., Allard, L. F., and Sun, Y. P. *J. Am. Chem. Soc.*, **2004**, *126*, 1014–1015.

[17] Tanigaki, T., Nishikiori, H., Kubota, S., Tanaka, N., Endo, M., and Fujii, T., *Chem. Phys. Lett.*, **2007**, *448*, 218–222.

[18] Hasobe, T., Fukuzumi, S., Kamat, and P. V. *J. Phys. Chem. B*, **2006**, *110*, 25477–25484.

[19] Huang, Y. Y., Ahir, S. V., and Terentjev, E. M. *Phys. Rev. B*, **2006**, *73*, 125422.

[20] Ahir, S. V., Terentjev, E. M., Lu, S. X., and Panchapakesan, B. *Phys. Rev. B*, **2007**, *76*, 165437.

[21] Ahir, S. V., Huang, Y. Y., and Terentjev, E. M., *Polymer*, **2008**, *49*, 3841–3854.

[22] Birkin, P. R., Offin, D. G., Joseph, P. F., and Leighton, T. G., *J. Phys. Chem. B*, **2005**, *109*, 16997–17005.

[23] Paulusse, J. M. J., and Sijbesma, R. P., *J. Polym. Sci. A*, **2006**, *44*, 5445–5453.

[24] S.S. Xie, W.Z. Li, Z.W. Pan, B.H. Chang, & L.F. Sun, *J. Phys. Chem. Sol.*, **2000**, *61*, 1153–1158.

[25] Collman, J. P., Elliott, C. M., Halber, T. R., and Tovrog, B. S. *Proc. Natl. Acad. Sci.*, **1977**, *74*, 18–22.

[26] Lin, V. S. Y., DiMagno, S. G., and Therien, M. J. *Science*, **1994**, *264*, 1105–1111.

[27] Chen, J., Liu, H. Y., Weimer, W. A., Halls, M. D., Waldeck, D. H., and Walker, G. C. *J. Am. Chem. Soc.*, **2002**, *124*, 9034–9035.

[28] Kong, J., and Dai, H. J. *J. Phys. Chem. B*, **2001**, *105*, 2890–2893.

[29] Sun, Y., Wilson, S. R., and Schuster, D. I. *J. Am. Chem. Soc.*, **2001**, *123*, 5348–5349.

[30] Chattopadhyay, D., Galeska, I., and Papadimitrakopoulos, F. *J. Am. Chem. Soc.*, **2003**, *125*, 3370–3375.

[31] Beigbeder, A., Linares, M., Devalckenaere, M., Degee, P., Claes, M., Beljonne, D., Lazzaroni,

R., and Dubois, P. *Adv. Mater.*, **2008**, *20*, 1003–1007.

[32] Povey, M. J. W., Hindlea, S. A., Kennedya, J. D., Steca, Z., and Taylorb, R. G. *Phys. Chem. Chem. Phys.*, **2003**, *5*, 73–78.

[33] Zhang, D., Ryu, K., Liu, X., Polikarpov, E., Ly, J., Tompson, M. E., and Zhou, C. *Nano Lett.*, **2006**, *6*, 1880–1886.

[34] Giordani, S., Bergin, S. D., Nicolosi, V., Lebedkin, S., Kappes, M. M., Blau, W. J., and Coleman, J. N. *J. Phys. Chem. B*, **2006**, *110*, 15708–15718.

[35] Wang, D., Ji, W X., Li, Z C., and Chen, L. *J. Am. Chem. Soc.*, **2006**, *128*, 6556–6557.

[36] Casey, J. P., Bachilo, S. M., and Weisman, R. B. *J. Mater. Chem.*, **2008**, *18*, 1510–1516.
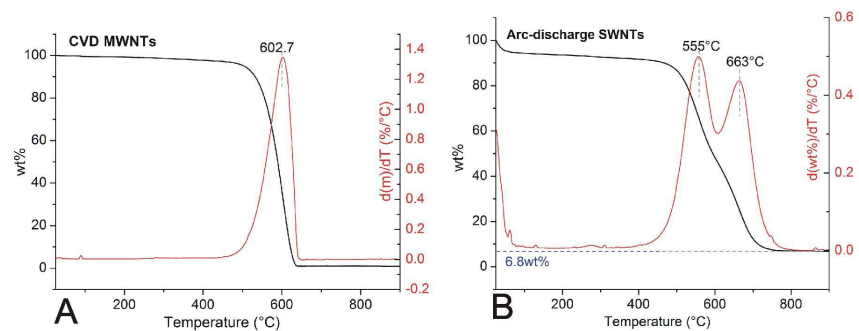
Supplementary Information

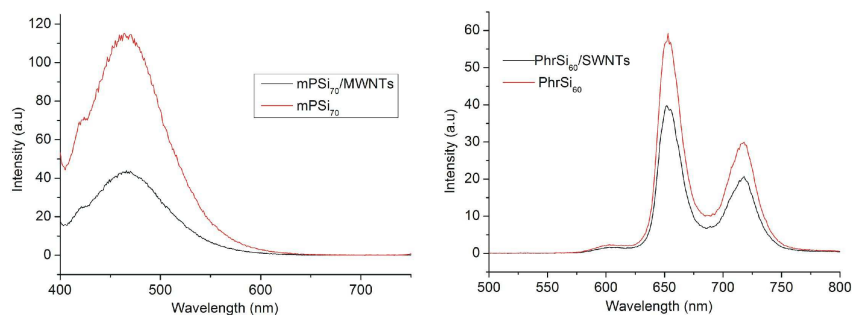FIG. 7: (A) Thermo-gravimetric analysis (TGA) of MWNTs; (B) TGA of SWNTs

FIG. 8: Left panel: plot showing fluorescence spectra of mPSi$_{70}$-PET reference solution, and mPSi$_{70}$/MWNT-PET solution; Right panel: plot showing fluorescence spectra of PhrSi$_{60}$-PET reference solution, and PhrSi$_{60}$/MWNT-PET solution